## A new class of Hanbury-Brown/Twiss parameters

Urs Achim Wiedemann and Ulrich Heinz Institut für Theoretische Physik, Universität Regensburg, D-93040 Regensburg, Germany (September 6, 2018)

In heavy ion collisions resonances can create strong non-Gaussian effects in the 2-pion correlation data. Hence, the commonly used Gaussian fit parameters do not fully characterize these correlators. We suggest a different set of HBT parameters which does not presuppose a particular shape of the correlator and allows to extract additional (non-Gaussian) information. Within a simple model for an expanding source including resonance decays it is shown that this additional information provides a clean distinction between scenarios with the and without transverse flow.

PACS numbers: 25.75.+r, 07.60.ly, 52.60.+h

The aim of Hanbury-Brown/Twiss (HBT) interferometric analyses of heavy ion collisions is to extract from the measured 2-particle correlators  $C(\mathbf{q}, \mathbf{K})$  of identical particles as much information as possible about the patio-temporal distribution S(x, K) of the particle emitting sources in the collision region. It is based on the relation [1,2]

Epatio-temporal distribution 
$$S(x, K)$$
 of the particle emitting sources in the collision region. It is based on the relation [1,2]
$$C(\mathbf{p}_1, \mathbf{p}_2) = 1 + \frac{\left|\int d^4x \, S(x, K) \, e^{iq \cdot x}\right|^2}{\left|\int d^4x \, S(x, K)\right|^2},$$

$$q = p_1 - p_2, \qquad K = \frac{1}{2}(p_1 + p_2). \qquad (1)$$
The particle emittends of the par

So far, the interplay between the experimentally measurable momentum correlator  $C(\mathbf{q}, \mathbf{K})$  and the theoretical concept of space-time emission function S(x, K) was inestigated mainly in the context of Gaussian approximations for both. Experimental data are commonly fit to a Gaussian ansatz [3]

$$C(\mathbf{q}, \mathbf{K}) = 1 + \lambda(\mathbf{K}) e^{-q_i q_j R_{ij}^2(\mathbf{K})},$$
 (2a)

$$R_{ij}(\mathbf{K}) = \begin{pmatrix} R_o^2 & R_{os}^2 & R_{ol}^2 \\ R_{os}^2 & R_s^2 & R_{sl}^2 \\ R_{ol}^2 & R_{sl}^2 & R_l^2 \end{pmatrix}, \qquad i, j = o, s, l. \quad (2b)$$

Here, the relative momentum components are defined parallel to the beam (l = longitudinal), parallel to the transverse component of  $\mathbf{K}$  (o = out), and in the remaining third direction (s = side).  $R_{os} = R_{sl} = 0$  for azimuthally symmetric collisions.

The fit parameters  $R_{ij}^2(\mathbf{K})$  can be calculated from a Gaussian ansatz for the emission function S(x,K) in terms of space-time variances  $\langle \tilde{x}_{\mu} \tilde{x}_{\nu} \rangle$  [4,5]:

$$S(x,K) \simeq N(K) S(\bar{x},K) e^{-\frac{1}{2}\tilde{x}^{\mu}\tilde{x}^{\nu}B_{\mu\nu}(\mathbf{K})},$$
 (3a)

$$(B^{-1})_{\mu\nu} = \langle \tilde{x}_{\mu}\tilde{x}_{\nu} \rangle, \ \tilde{x}_{\mu} = x_{\mu} - \bar{x}_{\mu}, \ \bar{x}_{\mu} = \langle x_{\mu} \rangle, \tag{3b}$$

$$\langle f(x) \rangle = \langle f(x) \rangle (K) = \frac{\int d^4x \, f(x) \, S(x, K)}{\int d^4x \, S(x, K)} \,.$$
 (3c)

In the resulting expression for the correlator,

$$C(\mathbf{q}, \mathbf{K}) = 1 + \exp\left(-q^{\mu} q^{\nu} \langle \tilde{x}_{\mu} \tilde{x}_{\nu} \rangle\right) , \qquad (4)$$

only three of the four relative momentum components are independent, the fourth being fixed via the on-shell constraint  $q^0 = \mathbf{q} \cdot (\mathbf{K}/K^0) = \mathbf{q} \cdot \boldsymbol{\beta}$ . In the Gaussian framework, the consequences of the on-shell constraint are well studied. Especially, the HBT radius parameters read [3,6]

$$R_{ij}^{2}(\mathbf{K}) = \langle (\tilde{x}_{i} - \beta_{i}\tilde{t})(\tilde{x}_{j} - \beta_{j}\tilde{t}) \rangle.$$
 (5)

This is the starting point of most spatio-temporal interpretations of correlation data. Note however that (6) presupposes a Gaussian shape of  $C(\mathbf{q}, \mathbf{K})$  since (6) determines the curvature components of the correlator at  $\mathbf{q} = 0$  [3]:

$$R_{ij}^{2}(\mathbf{K}) = -\left. \frac{\partial^{2} C(\mathbf{q}, \mathbf{K})}{\partial q_{i} \partial q_{j}} \right|_{\mathbf{q}=0}, \tag{6}$$

and these coincide with the experimentally determined half widths of  $C(\mathbf{q}, \mathbf{K})$  only for Gaussian correlators. Non-Gaussian characteristics of the correlator are difficult to quantify and control in this Gaussian framework.

Here, we suggest to characterize the correlator with a different set of a few HBT parameters, so-called q-moments, whose extraction does not presuppose a particular shape of  $C(\mathbf{q}, \mathbf{K})$ .

The HBT parameters used in the Gaussian framework are based on space-time variances  $\langle \tilde{x}_{\mu} \tilde{x}_{\nu} \rangle$ , i.e. on expectation values  $\langle f(x) \rangle$  of the emission function in coordinate space, cf. (3c). In contrast, we suggest here to base a quantitative analysis of  $C(\mathbf{q}, \mathbf{K})$  on q-variances which are expectation values  $\langle g(\mathbf{q}) \rangle$  of the true correlator  $C(\mathbf{q}, \mathbf{K}) - 1$  in relative momentum space.

For a Gaussian correlator, the HBT parameters can be determined either by fitting to the Gaussian (2), or by computing the integrals

$$\langle \langle q_i q_j \rangle \rangle = \frac{\int d^3 q \ q_i \ q_j \ [C(\mathbf{q}, \mathbf{K}) - 1]}{\int d^3 q \ [C(\mathbf{q}, \mathbf{K}) - 1]} = \frac{1}{2} \left( R^{-1}(\mathbf{K}) \right)_{ij}, \quad (7)$$

$$\lambda = \sqrt{\det R(\mathbf{K})/\pi^3} \int d^3q \left[ C(\mathbf{q}, \mathbf{K}) - 1 \right]. \tag{8}$$

For a non-Gaussian correlator, we can define the HBT radius parameters and the intercept  $\lambda$  in terms of these "q-variances".

The deviations of the correlator from a Gaussian shape ("non-Gaussicities") are then quantified by higher order q-moments. Due to the  $\mathbf{q} \rightarrow -\mathbf{q}$  symmetry of  $C(\mathbf{q}, \mathbf{K})$  the first non-Gaussian contribution shows up in the fourth order q-moments ("kurtosis"). All higher order q-moments can be calculated as derivatives of the generating function  $Z(\mathbf{y}, \mathbf{K})$ ,

$$Z(\mathbf{y}, \mathbf{K}) = \int d^3q \, e^{i\mathbf{q} \cdot \mathbf{y}} \left[ C(\mathbf{q}, \mathbf{K}) - 1 \right], \tag{9}$$

$$\langle \langle q_{i_1} q_{i_2} ... q_{i_n} \rangle \rangle = (-i)^n \frac{\partial^n}{\partial y_{i_1} \partial y_{i_2} ... \partial y_{i_n}} \ln Z(\mathbf{y}, \mathbf{K}) \Big|_{\mathbf{y} = 0} .$$
 (10)

¿From this generating function, the correlator can be reconstructed completely. The series of n-th q-variances (10) is merely a convenient way to characterize its shape starting with its "Gaussian" widths  $\langle \langle q_i q_j \rangle \rangle$  and going for increasing n step by step to finer structures.

To calculate  $Z(\mathbf{y}, \mathbf{K})$  directly from a given emission function it is convenient to use the normalized "relative distance distribution"

$$\rho(u;K) = \int d^4 X \, s(X + \frac{u}{2}, K) \, s(X - \frac{u}{2}, K) \,,$$

$$\int d^4 u \, \rho(u;K) = 1 \,, \tag{11}$$

written in terms of the normalized emission function  $s(x,K) = S(x,K)/\int d^4x \, S(x,K)$ .  $\rho$  is real and even in u. Then

$$Z(\mathbf{y}, \mathbf{K}) = \int d^3q \, e^{i\mathbf{q}\cdot\mathbf{y}} \, \int d^4u \, e^{iq\cdot u} \, \rho(u; K) \,. \tag{12}$$

In the Cartesian parametrization, this expression simplifies to a one-dimensional integral:

$$Z(\mathbf{y}, \mathbf{K}) = \int dt \, \rho(y_s, y_o + \beta_{\perp} t, y_l + \beta_l t, t; K) \,. \tag{13}$$

For Gaussian emission functions Eqs. (7), (10) and (13) reproduce the relations (5).

The method of q-variances generally requires to invert the matrix (7) and to discuss a 4-dimensional tensor of fourth order moments. Such a full analysis will be published elsewhere [7]. Here, we restrict ourselves to a unidirectional analysis of the correlations  $\tilde{C}(q_i, \mathbf{K}) \equiv C(q_i, q_{j\neq i} = 0, \mathbf{K})$  along the three Cartesian axes. For the relative momentum component  $q_i$ , the corresponding HBT radius parameter and intercept are then defined via the relations (we use the same notation as for the three-dimensional q-moments)

$$R_i^2(\mathbf{K}) = \frac{1}{2\langle\langle q_i^2 \rangle\rangle},$$
 (14a)

$$\langle\!\langle q_i^2 \rangle\!\rangle = \frac{\int dq_i \, q_i^2 \left[ \tilde{C}(q_i, \mathbf{K}) - 1 \right]}{\int dq_i \left[ \tilde{C}(q_i, \mathbf{K}) - 1 \right]}, \tag{14b}$$

$$\lambda_i(\mathbf{K}) = (R_i(\mathbf{K})/\sqrt{\pi}) \int dq_i \left[ \tilde{C}(q_i, \mathbf{K}) - 1 \right].$$
 (14c)

Even Gaussian correlators have non-vanishing higher q-moments:

$$\langle \langle q_i^{2m} \rangle \rangle^{\text{Gauss}} = \frac{(2m-1)!!}{(2R_i^2)^m}.$$
 (15)

Being expressible in terms of the second moments they do not contain new information. The non-trivial higher order information is contained in the (normalized) q-cumulants, in which these trivial contributions are subtracted:

$$\Delta_i^{(2m)} = \frac{1}{(2m-1)!!} \frac{\langle \langle q_i^{2m} \rangle \rangle}{\langle \langle q_i^2 \rangle \rangle^m} - 1.$$
 (16)

The normalization removes the dependence on the Gaussian widths of  $C(\mathbf{q}, \mathbf{K})$  and turns them into dimensionless measures for deviations from a Gaussian shape.

To extract the moments  $\langle\langle q_i^n\rangle\rangle$  from data one replaces (14b) by a ratio of sums over bins in the  $q_i$ -direction. The higher the order n of the q-moment, the more sensitive are the extracted values to statistical and systematic uncertainties in the region of large  $q_i$ . First investigations with event samples generated by the VENUS event generator indicate that the current precision of the data in the Pb-beam experiments at the CERN SPS permits to determine the second and fourth order q-moments [7]. Accordingly, we restrict our discussion of non-Gaussian features to the "kurtosis"

$$\Delta_i = \frac{\langle \langle q_i^4 \rangle \rangle}{3 \langle \langle q_i^2 \rangle \rangle^2} - 1. \tag{17}$$

We have computed the unidirectional Gaussian parameters  $R_i$  and the kurtosis  $\Delta_i$  for a model pion emission function including resonance decay channels R:

$$S_{\pi}(x,p) = S_{\pi}^{\text{dir}}(x,p) + \sum_{P} S_{R \to \pi}(x,p).$$
 (18)

The contributions  $S_{R\to\pi}$  are obtained from the direct resonance emission function  $S_R^{\rm dir}(X,P)$  by propagating the resonances of widths  $\Gamma$ , produced at  $(X_\mu,P_\mu)$ , along a classical path  $x^\mu=X^\mu+\frac{P^\mu}{M}\tau$  according to an exponential decay law [8,9]:

$$S_{R\to\pi}(x;p) = M \int_{s_{-}}^{s_{+}} ds \, g(s) \int \frac{d^{3}P}{E_{P}} \, \delta(P \cdot p - ME^{*})$$

$$\times \int d^{4}X \int d\tau \, \Gamma e^{-\Gamma\tau} \, \delta^{(4)} \left(x - \left(X + \frac{P}{M}\tau\right)\right)$$

$$\times S_{P}^{\text{dir}}(X, P) \,. \tag{19}$$

We consider isotropic decays in the resonance rest frame with decay phase space g(s),  $E^*$  being the energy of the

observed decay pion in this frame and s the squared invariant mass of the (n-1) unobserved decay products.

Our model assumes local thermalization at freeze-out and produces hadronic resonances by thermal excitation. For particle species i with spin degeneracy  $2J_i + 1$ , the emission function reads [4]

$$S_i^{\text{dir}}(x, P) = \frac{2J_i + 1}{(2\pi)^3} P \cdot n(x) \exp\left(-\frac{P \cdot u(x) - \mu_i}{T}\right) H(x),$$

$$H(x) = \exp\left(-\frac{r^2}{2R^2} - \frac{\eta^2}{2(\Delta\eta)^2} - \frac{(\tau - \tau_0)^2}{2(\Delta\tau)^2}\right). \quad (20)$$

The Boltzmann factor  $\exp[-(P \cdot u(x) - \mu_i)/T]$  implements both the assumption of thermalization, with temperature T and chemical potential  $\mu_i$ , and collective expansion with hydrodynamic flow 4-velocity  $u_{\mu}(x)$ . Space-time is parametrized via longitudinal proper time  $\tau = \sqrt{t^2 - z^2}$ , space-time rapidity  $\eta = \frac{1}{2} \ln \left[ (t+z)/(t-z) \right]$ , transverse radius r and azimuthal angle  $\phi$ . The Gaussian factors in H(x) specify the spatial extension of the source as well as a Gaussian average around a mean freeze-out proper time  $\tau_0$  with dispersion  $\Delta \tau$ . For freeze-out along proper time hyperbolas  $P \cdot n(x) = M_{\perp} \cosh(Y - \eta)$  [4] where Y and  $M_{\perp}$  are the rapidity and transverse mass associated with P.

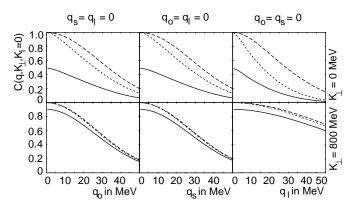


FIG. 1. Two-pion correlations for transverse flow  $\eta_f = 0$ . Curves are calculated for the model emission function (20) without resonance decay contributions (dashed lines), including pions from the shortlived resonances  $\rho$ ,  $\Delta$ ,  $K^*$ ,  $\Sigma^*$  and from the  $\omega$  (dotted lines), and including also pions from the longlived resonances  $\eta$ ,  $\eta'$ ,  $K_S^0$ ,  $\Sigma$ ,  $\Lambda$  (solid lines).

In the longitudinal direction we assume scaling expansion,  $v_l = z/t$  or  $\eta_l = \frac{1}{2} \ln[(1+v_l)/(1-v_l)] = \eta$ . For the transverse expansion we choose a linear rapidity profile:

$$\eta_t(r) = \eta_f\left(\frac{r}{R}\right). \tag{21}$$

All numerical results presented here are obtained for the set of source parameters T=150 MeV, R=5 fm,  $\Delta \eta=1.2, \tau_0=5$  fm/c,  $\Delta \tau=1$  fm/c and  $\mu_B=\mu_S=0$ . We include all pion decay channels of  $\rho$ ,  $\Delta$ ,  $K^*$ ,  $\Sigma^*$ ,  $\omega$ ,

 $\eta, \eta', K_S^0, \Sigma$  and  $\Lambda$  with branching ratios larger than 5 percent [10].

For this model we have numerically computed the 2-pion correlator. Typical results are shown in Fig. 1. A detailed model study of how resonance contributions affect the shape and pair momentum dependence of the correlator will be published elsewhere [11]. Here, we merely observe that due to their exponential decay law, resonance decays can contribute exponential tails to the emission function  $S_{R\to\pi}$  in (19), thereby leading to a generically non-Gaussian shape of the correlator.

To illustrate the use of q-variances we now discuss how the space-time characteristics of the emission region, specified in our model by the geometric input parameters and the transverse flow  $\eta_f$ , show up in these new 2-particle observables. First, we checked that for the model (18-20) the inverted second q-moments  $R_i$  coincide in all three directions i=0,s,l with the Gaussian fit parameters extracted for a set of n equidistant points  $q_i^{(j)}$  between 0 and 50 MeV by minimizing

$$\sum_{i=1}^{n} \left( \ln \tilde{C}(q_i^{(j)}, \mathbf{K}) - \log \lambda + R_i^2 q_i^{(j)^2} \right) = min.$$
 (22)

These "Gaussian" radius parameters  $R_i$  and their transverse momentum dependence is well-studied for model emission functions (20) not including resonance decay contributions [5]. Especially, it is known that the transverse homogeneity length  $R_t$  of (20), i.e. the size of the effective emission region in the transverse plane, shrinks with transverse flow  $\eta_f$  approximately like [5]

$$R_t \approx R \left( 1 + \frac{M_\perp}{T} \eta_f^2 \right)^{-\frac{1}{2}}.$$
 (23)

This introduces an  $\eta_f$ -dependent  $K_\perp$ -slope of  $R_s$  which was interpreted previously as a signature of transverse flow. Fig. 2 shows that if resonance decay contributions are added in the calculation, this distinctive behaviour is lost:  $R_s$  develops a  $K_\perp$ -slope even for scenarios without transverse flow. The reason is that resonances can propagate outside of the thermally equilibrated region before decaying. This effect ("lifetime effect") leads to exponential tails in  $S_{R\to\pi}$  and tends to increase the Gaussian widths  $R_i$ . Since the relative abundance of resonances is larger for small  $K_\perp$ , this tail is more pronounced in the region of small  $K_\perp$ , thereby leading to a  $K_\perp$ -slope of  $R_s$ .

In contrast, for a finite transverse flow  $\eta_f = 0.3$  the  $K_{\perp}$ -dependence of  $R_s$  is due to the flow, and resonance decay contributions do not change the slope of  $R_s$  in our model. This can be traced back to the shrinking transverse size (23) of the direct resonance emission function  $S_R^{dir}$  in (20): due to their larger rest mass, parent resonances have a smaller effective emission region than thermal pions in the transverse direction. For the case depicted in Fig. 2, this effect counterbalances the lifetime effect almost exactly.

According to (23), the absolute size of the *side* radius depends not only on  $\eta_f$  but also on the input parameter R for which no independent measurement exists. As a consequence, the Gaussian radius parameter  $R_s(K_\perp)$  by itself does not allow to distinguish scenarios with and without transverse flow once resonance decays are included. This conclusion extends to the other Gaussian widths,  $R_o$  and  $R_l$ , as well.

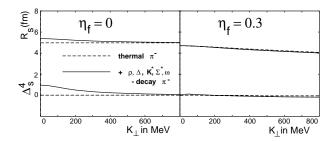


FIG. 2. The inverted q-variance  $R_s$  of (2.8a) and the kurtosis  $\Delta_s$  of (2.11) in the side direction at Y=0 as functions of  $K_{\perp}$ . Left:  $\eta_f=0$  (no transverse flow). Right:  $\eta_f=0.3$ . The difference between the dashed and solid curves is entirely dominated by  $\omega$  decays.

However, the physical origin of the  $K_{\perp}$ -slope of  $R_s$ is different for the two situations shown in Fig. 2. This shows up in the kurtosis of the corresponding correlators: without transverse flow, resonance decay contributions increase  $R_s$  due to the lifetime effect which generates exponential tails in  $S_{R\to\pi}$ . These tails manifest themselves in the correlator through a significant non-Gaussian component. For non-zero transverse flow, on the other hand, the  $K_{\perp}$ -slope arises from the  $K_{\perp}$ -dependent shrinking (23) of the effective transverse emission region. This effect is more prominent for resonances than for thermal pions, i.e.  $S_{\pi}^{dir}$  is spatially more extended in the transverse plane than  $S_R^{dir}$ , and hence it "covers" a substantial part of the exponential tails of  $S_{R\to\pi}$ . As a consequence, the total emission function (18) can be expected to show much smaller deviations from a Gaussian shape for the scenario with transverse flow, and this again leads to a more Gaussian correlator.

This explains why the kurtosis  $\Delta_s(K_\perp)$  plotted in Fig. 2 provides a clearcut distinction between the two scenarios.  $\Delta_s$  simply reflects the importance of resonance decays. For vanishing transverse flow,  $\Delta_s$  is significant and decreases with increasing  $K_\perp$  since the relative abundance of resonance decay pions dies out; for finite transverse flow  $\eta_f=0.3$ , it is an order of magnitude smaller. A  $K_\perp$ -dependence of  $R_s$  without measurable kurtosis is thus a clear sign of transverse flow.

Here, we do not discuss to what extent this particular  $\eta_f$ -dependence of the kurtosis  $\Delta_s$  is generic for realistic models of heavy ion collisions including resonance decays. This will require a more systematic study [11]. We simply conclude that higher order q-variances can provide cru-

cial additional information on the correlator which can help to distinguish physical scenarios which are difficult to disentangle on the level of "Gaussian" HBT radius parameters. On the other hand, they can still be directly related to specific features of the emission function and thus should aid the spatio-temporal interpretation of correlation measurements. This is less straightforward if one only knows the overall shape of the correlator, without decomposing it into its moments.

In summary, we expect these new HBT parameters, both the one- and multi-dimensional q-moments of the correlator, to become valuable additional observables in future comparisons between models and experiment.

This work was supported by BMBF, DFG and GSI. Discussions with P. Foka, H. Kalechofsky, B. Lasiuk, M. Martin, H.-P. Naef, L. Rosselet, P. Seyboth and S. Voloshin are gratefully acknowledged.

- E. Shuryak, Phys. Lett. B44, 387 (1973); Sov. J. Nucl. Phys. 18, 667 (1974).
- [2] S. Chapman and U. Heinz, Phys. Lett. B340, 250 (1994).
- [3] S. Chapman, P. Scotto and U. Heinz, Phys. Rev. Lett. 74, 4400 (1995); and Heavy Ion Phys. 1, 1 (1995).
- [4] S. Chapman, J.R. Nix and U. Heinz, Phys. Rev. C52, 2694 (1995).
- [5] U.A. Wiedemann, P. Scotto and U. Heinz, Phys. Rev. C53, 918 (1996).
- [6] M. Herrmann and G.F.Bertsch, Phys. Rev. C51 (1995), 328.
- [7] P. Foka, H. Kalechofsky and U.A. Wiedemann, in preparation.
- [8] P. Grassberger, Nucl. Phys. B120, 231 (1977).
- [9] B.R. Schlei et al., Phys. Lett. B293, 275 (1992); J. Bolz et al., Phys. Lett. B300, 404 (1993); and Phys. Rev. D47, 3860 (1993).
- [10] Particle Data Book, Phys. Rev. D50, 1173 (1994).
- [11] U.A. Wiedemann and U. Heinz, preprint TPR-96-14.